© APR 2026 | IRE Journals | Volume 9 Issue 10 | ISSN: 2456-8880
DOI: https://doi.org/10.64388/IREV9I10-1715885

Computational Exploration into The Antioxidant Activity of Some Phenolic Compounds Isolated from Moringa Oleifera Using Molecular Docking Studies, DFT Studies, Pharmacokinetics and Determination of Antioxidant Properties

HANNATU SANI [1], ABDULLAHI BELLO UMAR [2], BELLO ALIYU [3]
[1,2]*department Of Chemistry, Ahmadu Bello University, Zaria,*
[3] *State Key Laboratory of Oil & Gas Reservoir Geology and Exploitation, Chengdu University of Technology, Chengdu, China*

Abstract- ***Oxidative stress is a phenomenon caused by an imbalance between production and accumulation of oxygen reactive species (ROS) in cells and tissues. Antioxidants are known to play an important role in preventing diseases caused by oxidative stress such as cancer, heart disease, diabetes, stroke, rheumatoid arthritis, Alzheimer's disease, ageing, and cataracts. Natural antioxidants are considered safer and healthier compared with their synthetic origin. Most of the naturally available ones are phenolic compounds. Antioxidants having phenolic groups are the most widely used ones. Even while the hunt for antioxidant medications from plants has been the subject of numerous wet lab investigations, the high costs, high failure rates and lengthy development times have made this a challenge. Therefore, there is a need to propose a more effective approach to curb the aforementioned challenges. This research study pursues to propose a promising antioxidant drug candidate in an environment free of the challenges associated with the wet lab approach as mentioned earlier. The research findings identify four potential antioxidant candidates through molecular docking studies of some phenolic compounds isolated from Moringa oleifera. Geometric optimization performed using Spartan 14 software on the data collected from literatures and crystal structure of the protein enzyme retrieved from protein data bank (PDB ID:3WGX). The molecular docking simulation performed using molegro virtual docker provide four best hit compounds with higher docking scores than Ascorbic acid, the standard drug. The four best hit compounds are compound 9,4,10 and 8 with docking scores -138.04 kcal.mol-1, -123.399 kcal.mol-1, -117.287 kcal.mol-1 and -116.956 kcal.mol-1 respectively while the standard drug had a moldock score of -81.433 kcal.mol-1.Further screening of their physiochemical and ADMET properties using Lipinski, Ghose and Veber rules yield four best compounds with remarkable pharmacokinetics and non-toxicity. DFT calculations were also performed on the four lead compounds to investigate their quantum chemical parameters (Homo Lumo energy band gap, hardness, softness, electronegativity, chemical potential and elecrophilicity) which helps in understanding their physical and chemical properties, and the results revealed their higher reactivity than the standard drug. Due to the high efficiency of the computational approach, this research was able to probe into the radical scavenging potency of the phenolic groups present in the respective lead compounds and the results showed they have higher potency compared to the standard drug. Thus, the research concludes that these ligands can be further modelled into a more effective antioxidant in comparison to ascorbic acid, the standard drug.***

I. INTRODUCTION

1.1 Background

Oxidative stress is a phenomenon caused by an imbalance between production and accumulation of oxygen reactive species (ROS) in cells and tissues and the ability of a biological system to detoxify these reactive products [1]. ROS can play, and in fact they do it, several physiological roles (i.e., cell signaling), and they are normally generated as by-products of oxygen metabolism, despite this, environmental stressors (i.e., UV, ionizing radiations, pollutants, and heavy metals) and xenobiotics (i.e. antiballistic drugs) contribute to greatly increase ROS production, therefore causing the imbalance that leads to cell and tissue damage (oxidative stress) [1].

Antioxidants are molecules that can interact and inhibit the initiation or propagation of oxidation chain reactions which can cause damage to the cells of organisms or molecules [2]. Antioxidants can stop the chain reaction by stabilizing free radicals and blocking oxidation with others by oxidizing themselves [3]. Therefore, phenolic compounds are often reducing factors of oxidative stress [4].

Antioxidants are known to play an important role in preventing diseases caused by oxidative stress such as cancer, heart disease, diabetes, stroke, rheumatoid arthritis, Alzheimer's disease, ageing, and cataracts [5]. Antioxidants consist of synthetic antioxidants such as Butylated hydroxyanisole (BHA), Butylated hydroxytoluene (BHT), tert-butyl hydroquinone (TBHQ), propyl gallate, and natural antioxidants derived from plants [6]. Thus, natural antioxidants sourced from natural ingredients are extensively explored as alternative sources of antioxidants [5]. Synthetic antioxidants are cheap, stable, and effective and have undergone several toxicological tests. However, synthetic antioxidants are toxic, carcinogenic, and non-biodegradable and pose environmental problems. In addition, new regulations on applying synthetic antioxidants restrict their usage. Natural antioxidants are considered safer and healthier compared with their synthetic origin. A large number of natural antioxidants, more than nine hundred and eighty (980), have been identified as an alternative to their synthetic counterparts two decades ago [7]. Most of the naturally available ones are phenolic compounds. Antioxidants having phenolic groups are the most widely used ones. Natural antioxidants can be produced from vegetables, fruits, spices, herbs, nuts, oilseeds, cereals, legumes, animal and microbial sources [7].

1.2 Statement of Research Problem

Ageing, heart disease, and cancer are examples of oxidative damage that is getting more difficult to treat with current therapies [8]. New chemicals for the creation of drugs to cure various oxidative stress ailments can be found in plants [9]. Even while the hunt for antioxidant medications from plants has been the subject of numerous wet lab investigations, the high costs, high failure rates and lengthy development times have made this a challenge [10]. Additionally, there is little knowledge about the antioxidant potential of each phenolic group on an antioxidant compound, which aids in enhancing the radical scavenging capacity and hence in the development of improved antioxidant drugs [11]. Therefore, it is necessary for chemists to propose new, more efficient and cost-effective drug candidates [12]. Consequently, computational approaches have been employed for the fast design of new antioxidant drugs. This approach which uses computational methods to model drug receptor interactions in order to evaluate if a given chemical will attach to a target and with what affinity, effectively reduces the time required to obtain valuable drugs as well as the high-cost implication of new drug discovery [13]. Also, this computational method seeks to probe into the radical scavenging capacity of each phenolic group in a compound which is presently not possible for the wet lab chemists [14].

1.3 Justification

This research study seeks to not only propose novel potential antioxidant compounds with high radical scavenging capacity agents, but also to reduce the cost implications and the length of time associated with the wet lab method for the development of antioxidant drug. Additionally, this research seeks to probe into the radical scavenging capacity of each phenolic group in a compound which is presently not possible for the wet lab chemists.

1.4 Aim and objectives

The aim of this research study is to computationally analyze the antioxidant capacity and radical scavenging potency of eleven (11) phenolic compounds and identify the lead compound that has outstanding antioxidant characteristics as a possible medication against oxidative damage in the human body. The objectives listed below will be employed in order to achieve the research study's aim to:

- obtain from the chemical database a set of compounds with activity against oxidative stress-related damage (collection of data set).
- Use the Chem-Draw software in creating a two-dimensional (2D) structure of the compounds that were obtained.

- convert the drawn structures (in 2D) to three-dimension (3D) using the Spartan 14 software version 1.1.4 and minimize the energy of the structures using the MM2 Force field in the Spartan 14 software.
- carry out Geometrical optimization on the compounds using DFT/B3LYP approach and 6-311G* basis set
- retrieve the crystal structure of the Human Estrogen Receptor ligand-binding Domain (PDB ID: 3WGX) from the Protein Data Bank
- Dock the compounds in the active site of the Human Estrogen Receptor ligand-binding domain using MVD
- select the poses of the top scored conformation among the compounds and visualize them using Discovery studio
- predict the drug-likeness pharmacokinetic properties and identify the lead compound.

II. MATERIAL AND METHODS

2.1 Materials

The materials used include a system and a number of computer software packages.

2.1.1 System specification

The entire research work was carried out using a hp Laptop (DESKTOP-PCCPCN9) equipped with an Intel(R) Core (TM) i5-7200U CPU processor running at 2.50GHz and 8.00 GB RAM on windows 10. Operating system: 64-bit operating system, x64-based processor

3.1.2 Software packages used

The software packages used for this research include; ChemDraw version 12.0.2, Spartan "14 v 1.1.4, Molegro Virtual Docker (MVD) and Discovery Studio (DS).

In addition to these software packages, the SwissADME(http://www.swissadme.ch/) and pkCSM(https;//biosig.lab.uq.edu.au/pkcsm/prediction) online web tools were also utilized for evaluating the pharmacokinetics and ADMET properties of the compounds.

2.2 Methods

The steps and procedures involved in the computational method used for this research work are explained in this section as follows;

2.2.1 Ligand selection and sketching

Eleven (11) compounds were retrieved from Pubchemsssss. Two-dimensional (2D) structure of the compounds was drawn using ChemDraw software (version 12.0.2) as shown in table 1.0.

2.2.2 Ligand preparation and Geometric Optimization

The sketched 2D structures of all the compounds were imported to the Spartan 14 software interface, which enabled their transformation into 3D format. Energy minimization of the compounds (in their 3D format) was done using the MM2 force field in the spartan 14 to help the docking program detect the bioactive conformer from the local minima. Geometric optimization of the compounds was done using the Density Functional Theory (DFT) method at the B3LYP level of theory and 6-311+G* basis set in order to find the most stable conformer(s) of all the compounds. The results were then saved in a separate folder in PDB file format ready for docking.

2.2.3 Receptor (Protein) preparation and Molecular docking

The crystal structure of ERp46 Trx2 protein with PDB ID: 3WGX co-crystallized with its native ligands was downloaded from the Protein Databank at [15]. Ligand-binding domain was prepared with Molegro Virtual Docker 6.0 by updating the H-atoms and eliminating the water (excess) molecules found in the complex structure. The attached(native) ligands were also detached from the target. The potential ligand-binding cavities of the human protein receptor was predicted, and the binding cavity was set inside a restricted sphere of X:27.27,Y:23.61,Z:28.93 with radius of 29A having a grid resolution of 0.30A.

For the molecular docking, all the prepared compounds (ligands), including the ascorbic acid(reference-inhibitor), were imported into the Molegro Virtual Docker 6 while Discovery Studio (DS) Visualizer was adopted to visualize various intermolecular interactions.

2.2.4 Physico-Chemical and ADMET Biochemical Investigation

Selected compounds from the molecular docking analysis were assessed for their drug-like behavior through an online server (SwissADME), while the analysis of pharmacokinetic parameters required for absorption, distribution, metabolism, and excretion (ADME) was performed using the online server (pkCSM).

2.2.5 Density Functional Theory (DFT) Calculations

The electronic and structural properties of the four best hit compounds selected from the docking investigation were calculated using the DFT method at the B3LYP level of theory and 6– 311G* basis set aided by Spartan 14 software. The calculated parameters used in this study include the highest occupied molecular orbital (HOMO) and the lowest unoccupied molecular orbital (LUMO) energies, hardness, softness, electronegativity, chemical potential and electrophilicity index. The molecular electrostatic potential surfaces (MEPs) were obtained from the population analysis calculations and visualized using Spartan 14 software. These parameters play a significant role in elucidating the magnitude of ligands interaction in the binding pocket of the human protein receptor ligand-binding domain.

2.2.6 Calculation of DFT Equation Parameters

Energy bandgap (ΔE) = ELUMO-EHOMO ---------- (1)

Chemical hardness (η) = - 1/2(EHOMO-ELUMO) ----------(2)

Chemical softness (σ)= 1/η ---------- (3)

Global electronegativity (χ) = -((EHOMO + ELUMO))/2 ---------- (4)

Chemical potential (μ) = - χ ---------- (5)

Electrophilicity (ω) = χ^2/2η ---------- (6)

2.2.5 Calculation of antioxidant parameters

In order to evaluate the preferred mechanism of free radical scavenge, various antioxidant descriptors were calculated as presented below:

2.2.5.1 The Homolytic Bond Dissociation Enthalpy (BDE)

This is the standard enthalpy change at a given temperature when a particular chemical bond is broken under standard conditions. The stability of the corresponding hydroxyl group is determined by the value of the BDE. When the BDE value is low, the stability of the corresponding O–H bond is low and thus can easily be broken. This gives rise to high antioxidant capacity for the considered compound (Rajan et al., 2019). This parameter was calculated under standard conditions of 1 atm and 298.15 K as presented in Eq. 1.

BDE = Hradical + HH - Hneutral ---------- (1)

2.2.5.2 The Adiabatic Ionization Potential (AIP)

This potential describes the process of electron donation by the antioxidant. It represents the capacity of the antioxidant to transfer electrons to the free radical. The lower the AIP value for a given molecule, the easier is the capacity to transfer electrons and the higher the susceptibility of that molecule to undergo ionization. Molecules with high to low AIP values have been observed to possess very strong antioxidant properties (Rajan et al., 2019). This parameter was estimated according to Eq. 2;

AIP = Hcation radical + Helectron -Hneutral ---------- (2)

3.2.5.3 The Electron Transfer Enthalpy (ETE)

Eq. 5 was employed in the calculation of ETE. The lower the ETE value, the more active is the resulting phenoxide anion for a given molecule (Rajan et al., 2019).

Calculation of Antioxidant Equation Parameters

BDE = Hradical + HH - Hneutral ---------- (1)

AIP = Hcation radical + Helectron -Hneutral ---------- (2)

ETE = Hradical + Helectron - Hanion ---------- (4)

Where;

Hradical = Total enthalpy of phenoxyl radical.

HH = Total enthalpy of the hydrogen atom.

Hneutral = Total enthalpy of neutral compound.

© APR 2026 | IRE Journals | Volume 9 Issue 10 | ISSN: 2456-8880
DOI: https://doi.org/10.64388/IREV9I10-1715885

HH+ = Total enthalpy of the proton.
Hcation radical = Total enthalpy of the cation radical.
Helectron = Total enthalpy of the electron.
Hanion = Total enthalpy of the anion.

Table 1: Names and structures of the studies compounds

SN	COMMON NAME	STRUCTURE
1	Ferulic acid	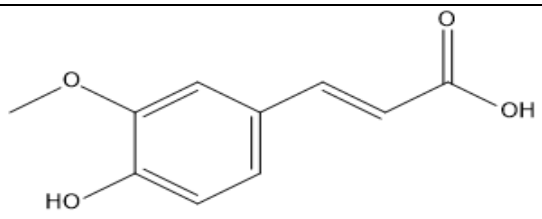
2	Gallic acid	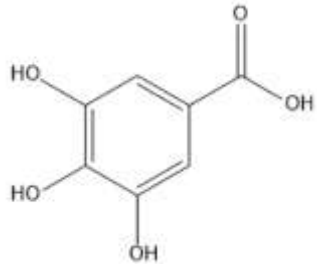
3	Caffeic acid	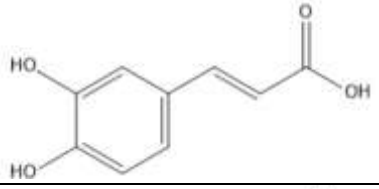
4	Chlorogenic acid	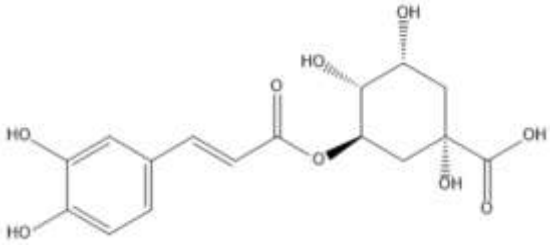
5	Ellagic acid	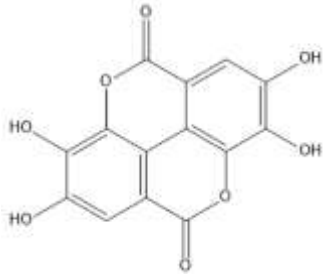
6	Kaempferol	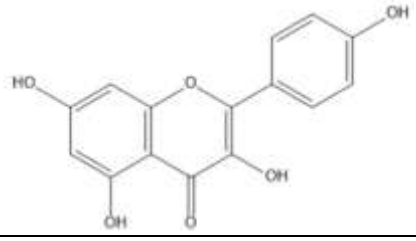

© APR 2026 | IRE Journals | Volume 9 Issue 10 | ISSN: 2456-8880
DOI: https://doi.org/10.64388/IREV9I10-1715885

7	Myricetin	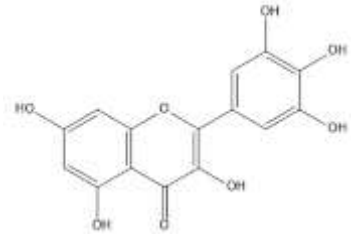
8	Quercetin	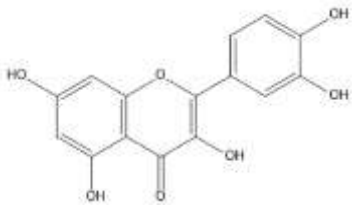
9	Isoquercitrin	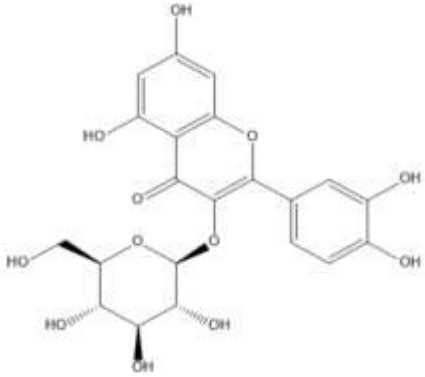
10	Luteolin	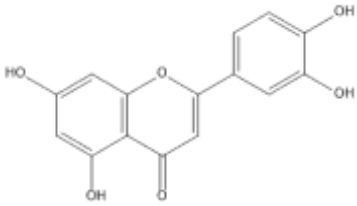
11	Vanillin	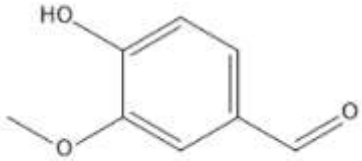

III. RESULT AND DISCUSSION

3.1 Molecular Docking Studies

Docking results of all the 11 studied ligands and the standard drug (ascorbic acid), into the binding pocket of the protein target, yielded the most potent drugs as shown in Table 1. The four best hit ligands were sorted by docking score in comparison to standard drug, and the chosen ligand binds to the target efficiently. The docking results for the top four hits (4,8,9 and 10) and their interactions with the protein target are presented in Table 1, and were further investigated to explore the performance of the outstanding docking scores.

The hydrogen atoms of the phenolic groups of ligand 4 (MolDock score: -123.399kcalmol-1 and Rerank score: -93.8559kcalmol-1) formed a conventional hydrogen bond interactions with GLU193 and GLU288 which have bond length of 1.76928 and 2.14284 .The hydrogen atom on the hydroxyl group attached to the cylohexane conserved residue SER197 and ALA196 which have bond lengths of 2.00727 and 3.05366 respectively.The oxygen

heteroatom conserved residue LYS280 and TYR277 which have bond legths of 1.85016 and 2.63887.Also,a C-Hbond is formed with the oxygen atocomplex m of the hydroxyl group attatched to the hydroxyl group of the cyclohexane via SER195. Others include Amide-Pi stacked interaction with LEU194. The hydrophobic and H-bonding interactions of target with the ligand may account for the excellent binding affinity (Fig. 1, complex 4).

In the docked complex of ligand 8 (MolDock score: -116.956kcalmol−1 , Rerank score: -105.146 kcalmol−1), the catechol moiety conserved residue GLN276 and ASPP275 with bond lengths of 1.8142 and 1.58957 respectively. Also, one of the phenolic groups of the catechol moiety formed a C-H bond with TYR277.The benzene ring of the with the catechol moiety formed a C-H bond via LYS278.The oxygen heteroatom of the complex 8 formed a C-H interaction with the target via TYR277 and GLY279. Furthermore, LYS28, TYR277, TYR277, HIS250 and HIS250 interacted with ligand 24 via pi-alkyl and pi-pi stacked hydrophobic interactions. The phenolic group conserved residue LYS280 (bond length of 2.72469) and also the carbonyl group formed an H-bond network via SER195 residue of bond length 2.34218.

The docking of ligand 9 in the binding site of the target (Fig. 2, complex9) yielded a MolDock score of --138.04 kcalmol−1 and a Rerank score of -128.925kcalmol−1, indicating strong interactions between the ligand and the receptor. The catechol moiety conserved residue GLN249 of bond length 2.05428. Also, the benzene ring of the catechol moiety formed a hydrophobic interaction with the moiety via an LYS278 pi-Alkyl residue. The enol group also forms a H-bond interaction with the target via SER285 (bond length: 1.82303). We observe more interaction on the single glucose moiety on carbon three of the C ring of quercetin backbone of ligand 9. The glucose moiety forms conventional H-bond interaction with the target via residues GLN276, SER197 and ALA196 with 2.01527, 1.66456 and 2.75786 bond lengths respectively. Also, the glucose moiety also forms a C-H bond via ASP275 and SER195 residue.

As shown in Table 1, the docked complex of ligand 10 in the binding pocket of target revealed excellent docking scores (MolDock score: -117.287kcalmol−1 and Rerank score: -102.519kcalmol−1). The phenolic group and the carbonyl group of the ligand interact with GLN276 (bond length: 1.82451) and LYS280 (bond length: 2.70425) via conventional hydrogen bonds. A C-H bond is also formed via LYS278 residue with the benzene ring bearing the phenolic group. Furthermore, the benzene ring has a hydrophobic interaction via pi-Alkyl and pi-pi Stacked bonds with LYS278, TYR277 and HIS250 residues.

H-bonding is a significant indicator of strong protein ligand interactions, and it frequently results in high binding affinity. The number of hydrogen bonds formed in protein-ligand interactions frequently increases the antioxidants radical scavenging potency against the target protein. Figures 1 and 2: show a 3D and 2D representation of the binding modes within the active site of the target protein. The formation of conventional hydrogen bonds between the chosen ligands and the target protein resulted in good ligand binding. Furthermore, as a standard comparable to the investigated ligands, the antioxidant drug (ascorbic acid), which also contains a hydroxyl group, carbonyl group, ether group, was used as a standard in this study, and all of the chosen ligands outperform ascorbic acid when docked into the same investigated protein receptor. Surprisingly, the ligands tested were a better free radical scavenger than ascorbic acid. The chosen ligands had a higher docking score, a more stable MolDock score, and a significantly lower Re-rank score than ascorbic acid.

Table 2: Docking results of the four best docked ligands

SN	MolDock score (kcal.mol-1)	Rerank score(kcalmol-1)	Einter(kcal.mol-1)	EHbond(kcal.mol-1)
9	-138.04	-128.925	-177.407	-16.1651
4	-123.399	-93.8559	-146.7	-5.9726

10	-117.287	-102.519	-137.639	-8.17149	Moldock score was obtained from the PLP scoring functions with a new H-bond term and extra charge schemes [1]. Rerank score is a linear combination of E-inter (Electrostatic, Van der Waals, H-bonding, steric) between the ligand and the protein target, and E-inter is the total dinteraction energy between the protein and the pose. EHbond is Hbond energy.
8	-116.956	-105.146	-138.189	-9.38267	
Standard drug	-81.433	-72.5979	-86.5827	-11.8816	

Table 3. Docking results of the four best docked ligands

SN	HYDROGEN BOND(HB)	Bond Length (Å) for HB	C-HBond	Alkyl	PiAlkyl	Pi-Pi Stacked	Pication/anion	PiSulphur
9	ALA196	2.75786	SER195		LYS278			
	SER197	2.51619	ASP275					
	SER197	1.66456						
	SER197	1.93374						
	SER285	1.82303						
	GLN249	2.05428						
	GLN276	2.01527						
4	ALA196	3.05366	SER195					
	TYR277	2.63887	TYR277					
	LYS280	1.85016						
	SER197	2.00727						
	GLU288	1.9248						
	GLU193	1.76928						
10	LYS280	2.70425			LYS278	TYR277		
	GLN276	1.82451				HIS250		
						HIS250		
8	SER195	2.34218	SER195*		LYS278	TYR277		
	LYS280	2.72469	TYR277			TYR277		
	ASP275	1.58957	GLY279			HIS250		
	GLN276	1.8142	TYR277			HIS250		
			LYS278					
Standard drug	SER195	2.121	SER197					
	SER197	2.86029	TYR289					
	SER292	2.35738	SER292					
	SER285	2.0734						

© APR 2026 | IRE Journals | Volume 9 Issue 10 | ISSN: 2456-8880
DOI: https://doi.org/10.64388/IREV9I10-1715885

Complex 9

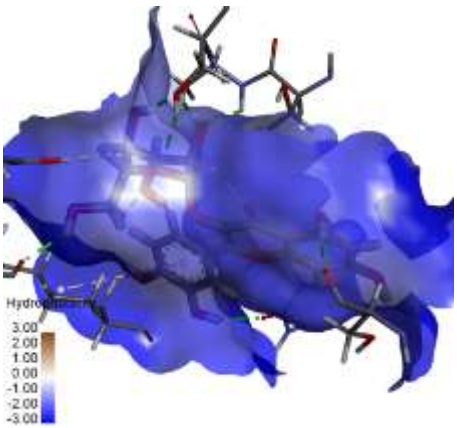

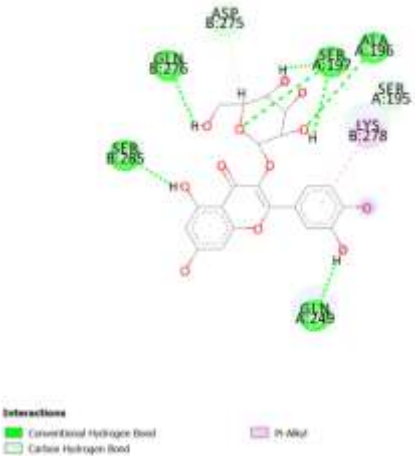

Complex 4

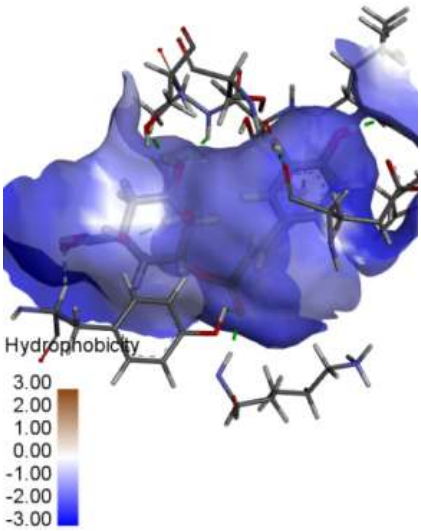

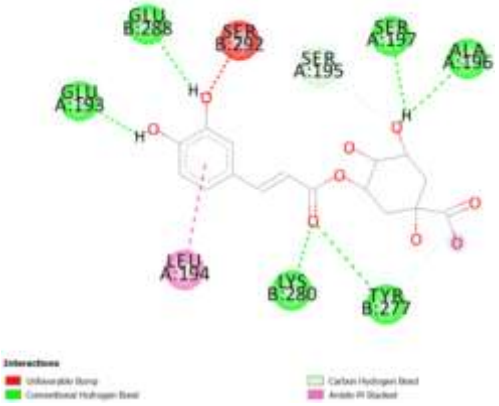

Complex 10

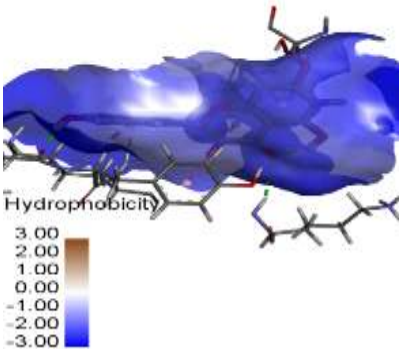

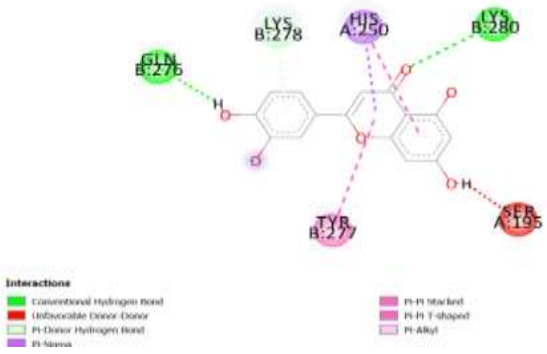

© APR 2026 | IRE Journals | Volume 9 Issue 10 | ISSN: 2456-8880
DOI: https://doi.org/10.64388/IREV9I10-1715885

Complex 8

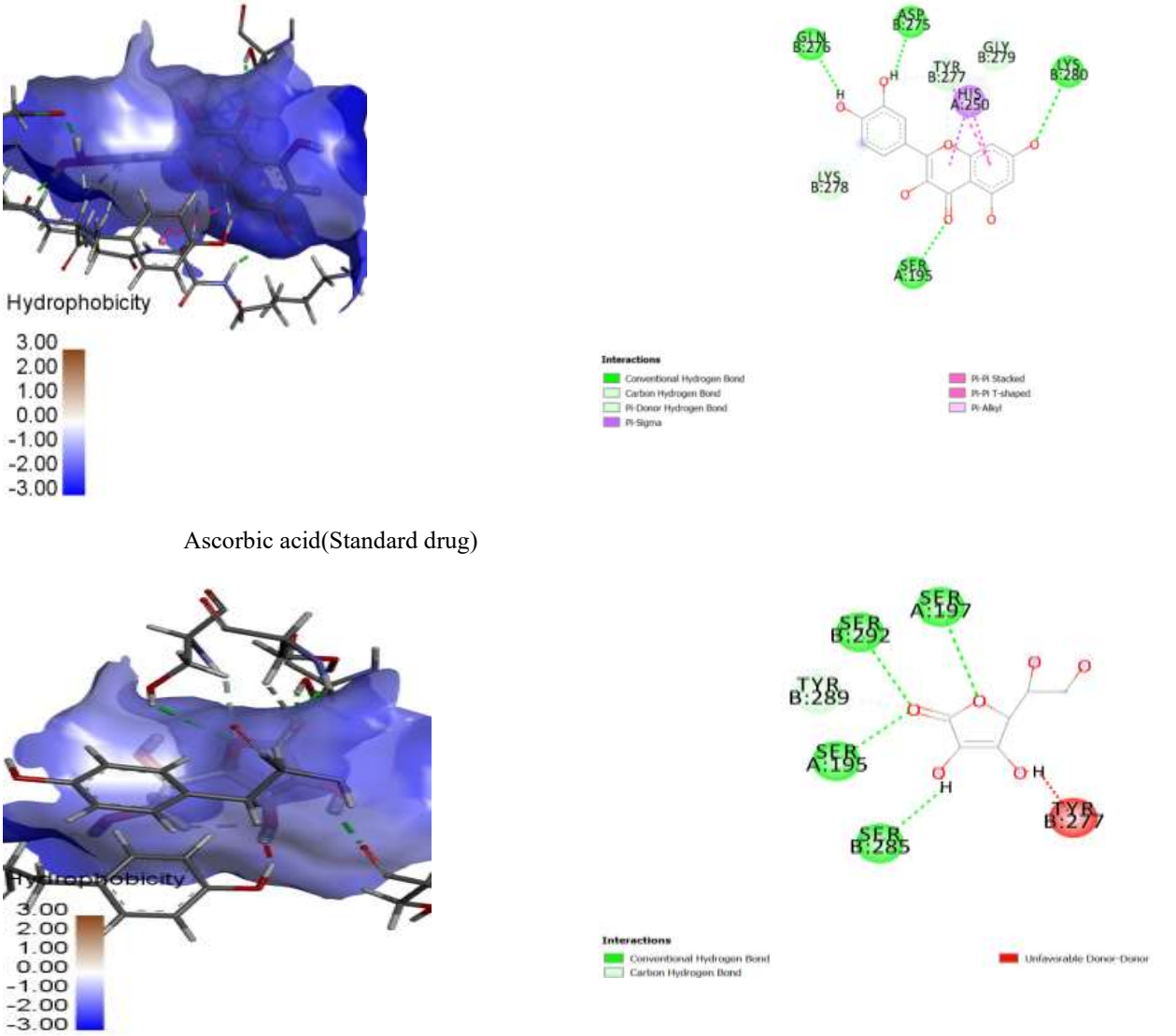

Ascorbic acid(Standard drug)

Figure 1. 3D and 2D representations for the interactions of the selected complexes (9,4,10 and 8)

4.2 Pharmacokinetic Studies

To further confirm that the selected compounds are possible drugs, their drug-likeness, and pharmacokinetics were determined. SwissADME and pkCSM web servers were used to perform drug-likeness analyses, and pharmacokinetic predictions for the investigated ligands. The predicted drug-likeness and pharmacokinetic properties are given in Tables 4.3 and 4.4. To make a comparison, drug-likeness analyses, and pharmacokinetic predictions were also performed for the reference drug (Ascorbic acid). Lipinski's rule suggests that good absorption occurs only when: the Mol. Wt. <500. The molecular weights of the investigated compounds were found to be in the range of 286.24to 464. 38gmol−1.We observe that all the selected compounds from obey the Lipinski rule. It also demonstrated that none of the investigated compounds have more than ten hydrogen bond acceptors, with compound 4 having the highest number of hydrogen bond acceptors with a value of five.

On the other hand, according to Ghose rule, the partition coefficient for a given molecule should be between −0.4 and 5.6. The average partition

coefficient of the selected ligands, which is the average of Log P, was predicted in the study to be in the range of -0.6459–2. 2824. We observe here that compound 4 and 9 have a Log P value of -0.6459 and -0.5389 respectively. This is an indicator that they do not obey the Ghose rule. Veber rule states that the topological polar surface area should not be greater than 140 Å2. The polar surface areas of the compound 8 and 10 obeyed this rule while compound 4 and 9 disobeyed the rule. The rotatable bonds in the molecule should follow the Veber and Muegge rules. The number of rotatable bonds in the molecule should not exceed 10 and 15, respectively. All of the mol ecules investigated in the study have rotatable bonds less than 10 and follow the Veber and Muegge rules. Using a value bioavailability score (ABS) criteria, the selected compound was further screened for an optimum profile of permeability and bioavailability. An ABS score of 0.55 indicates that the Lipinski rule is followed.

The studied ligands have intestinal absorption values ranging from 22.257-82.175%, indicating their ease of absorption. VDss denotes the apparent volume of distribution after enough time has passed for the drug to distribute uniformly through all tissues. A high VDss value (>0.5) indicates that the drug is well distributed in the plasma, whereas a low VDss value (-0.5) indicates that the drug is unable to cross the cell membrane. The predicted VDss value is between -1.357 and 0.672. This suggests that the ligands under consideration have a reasonable distribution in plasma. . Also, the BBB (blood-brain-barrier), and the penetrability to the CNS (central-nervous system) are essential factors in acquiring the optimum pharmacological drug. According to the standard scale of drug the BBB, and CNS penetrability standard values are shown as < -1 to >0.3 for log BB, and < -3 to > -2 for log PS. In a given ligand, the log BB of < -1 exhibits the insufficient diffusion of the drug molecule to the brain, whereas log BB value of >0.3 indicates that the drug molecule can cross the BBB, and log PS value of > -2 means that the drug molecule can enter the CNS, while < -3 suggests that it will be hard for the drug molecule to make it to the CNS. Results given in Table 4 revealed that only ligand 10 out of the four chosen ligands have demonstrated a high possibility to cross the barriers.

Cytochrome (CYP450) is a robust metabolic enzyme in the body of a human with five main isoforms: CYP2 D6, CYP3 A4, CYP A2, CYP2 C19, CYP2 C9, CYP2 D6 and CYP3 A4. Results in Table 4, indicated promising free radical scavenging capacity for the ligands and hence possess safe pharmacokinetic interactions. The dosing effect and bio-availability of a drug to reach steady-state concentrations is measured by clearance. A low value of clearance suggests increased endurance of a drug molecule in the body. All the chosen ligands demonstrated good acceptability in the body. Toxicity is used to decide whether a drug candidate is toxic or not. The result showed in table 4 show that all the selected compounds are nontoxic. As a result, it can be concluded that the selected ligands have the desired pharmacokinetic properties and can be used as potential antioxidant drugs in the future in the protein target used.

Table 4. Predicted Drug-likeness properties of the selected ligands

SN	Mol. Wt.	HBA	HBD	Log P	TPSA (Å2)	NRB	BA
4	354.31	5	9	-0.6459	164.75	5	0.11
8	302.24	1	7	1.988	131.36	1	0.55
9	464.38	4	12	-0.5389	210.51	4	0.17
10	286.24	1	6	2.2824	111.13	1	0.55
Standard drug	176.124	6	4	-1.4074	107.22	2	0.56

Mol. Wt.: molecular weight; HBA: hydrogen bond acceptor; HDB: hydrogen bond donor; NRB: number of rotatable bonds; TPSA: topological polar surface area, BA: Bioavailability Score.

© APR 2026 | IRE Journals | Volume 9 Issue 10 | ISSN: 2456-8880
DOI: https://doi.org/10.64388/IREV9I10-1715885

Table 5. Predicted ADMET properties of the selected ligands.

	Absorption	Distribution			Metabolism							Excretion	Toxicity
					Substrate		Inhibitor CYP						
SN	Intestinal Absorption	VDss (human)	BBB Permeability	CNS permeability	2D6	3A4	1A2	2C19	2C9	2D6	3A4	Total clearance	AMES toxicity
	Numeric (%absorbed)	Numeric (log L kg^{-1})	Numeric (log BB)	Numeric (log PS)				(yes/no)				Numeric (log mL min^{-1} kg^{-1})	(yes/no)
9	42.838	0.672	-1.755	-4.731	No	No	No	No	No	No	No	0.5	No
4	22.257	-1.357	-1.489	-3.948	No	No	No	No	No	No	No	0.325	No
10	82.175	-0.173	1.145	-2.405	No	No	Yes	No	Yes	No	Yes	0.568	No
8	75.347	-0.03	-1.339	-3.317	No	No	Yes	No	Yes	No	No	0.484	No
SD	39.716	-0.092	-1.031	-3.971	No	No	No	No	No	No	No	0.631	No

VDss: volume of distribution; BBB: blood-brain barrier; CNS: central nervous system; CYP: Cytochrome P

Ligand 9

Ligand 4

© APR 2026 | IRE Journals | Volume 9 Issue 10 | ISSN: 2456-8880
DOI: https://doi.org/10.64388/IREV9I10-1715885

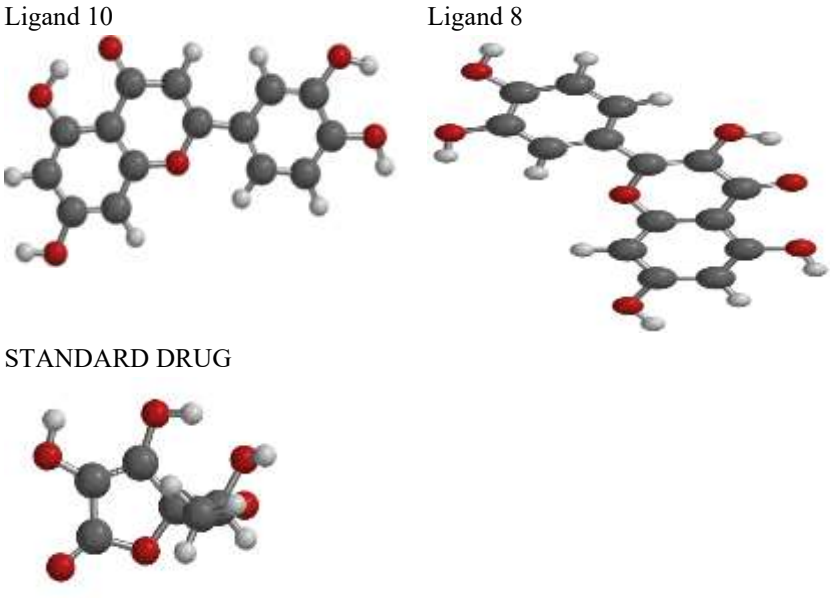

Figure 2. Optimized geometry of the selected ligands

3.3 DFT Studies

The Optimized geometries and the frontier molecular orbitals (HOMO, and LUMO illustrations) of the selected ligands achieved from DFT computations are given in Figs. 3 and 4. All of the geometry-optimized structures corresponded to a global minimum, according to the results. Frontier molecular orbitals (HOMO and LUMO diagrams) of the four-hit ligands specify a critical role in charge-transfer interactions with the V600E-BRAF binding site. As shown in Fig.3, the blue and red colors represent the orbital's positive and negative the orbital values. Furthermore, the shapes of the frontier orbitals can be used to determine reactivity. The HOMO is delocalized onto the phenolic groups, benzene rings, double bonds and the carbonyl groups. However,the distribution is primarily dominated at the benzene rings, phenolic groups and carbonyl groups. The blue region represents the maximum value of the HOMO, while the red region represents the minimum value. The HOMO electron density distribution of the studied ligands indicates that the ligands interact favorably with the protein target. Similarly, the LUMO delocalizes across the benzene rings, phenolic groups, and carbonyl groups also. However, we observe a larger distribution across the catechol moiety on ligand 9 and 10. The electronic surfaces of HOMO and LUMO revealed the benzene rings, phenolic groups and the carbonyl groups have the potential to interact with the target when the conditions are favorable. This typical behavior is appropriate for donor-acceptor interactions, which may be responsible for the ligands' excellent binding to the target.

Table 6 displays the HOMO and LUMO energies, as well as the Quantum chemical descriptors associated with the selected ligands. A good electron-donor molecule has a higher HOMO energy, whereas a lower energy value indicates a weak electron-acceptor [34]. Furthermore, a smaller energy gap between the LUMO and HOMO energies has a significant influence on intermolecular charge transfer and molecule bioactivity. As a result, a small energy gap observed in the hit ligands positively affects the electron's movement from the HOMO to the LUMO, resulting in a strong affinity of the drug to the target. The Egap value rises following the following:8(3.7 eV) vs. 9(4.14 eV) vs. 4(4.16 eV) vs. 10(4.17 eV). As energy gap values decrease, the order of reactivity increases.

The η (hardness) and the σ (softness) are significant reactivity variables for the behavior of a ligand in a chemical system. A hard molecule always has a higher resistance to altering its electronic dispersal during a chemical reaction, while a soft molecule has a lower resistance to altering its electronic-

© APR 2026 | IRE Journals | Volume 9 Issue 10 | ISSN: 2456-8880
DOI: https://doi.org/10.64388/IREV9I10-1715885

distribution in a reaction. Results from Table 3 indicated a high η value with a low σ value compared to analogous reported molecules. The χ (electronegativity) of a given molecule determines its capacity for electron attraction. The χ was computed to be around 3.6 to 4.04 eV, describing them as donor-electrons. The μ (chemical-potential) values for all of the selected ligands are negative, indicating good stability and the formation of a stable complex with the receptor. The ω (electrophilicity) of a molecule predicts the electrophilic nature and measures the tendency to accept an electron. The position of organic molecules based on the ω values follows the order; ω1.5 eV, revealed strong electrophiles. As a result, the calculated electrophilicity value identifies the selected ligands weak electrophiles.

HOMO	LUMO
Ligand 9	
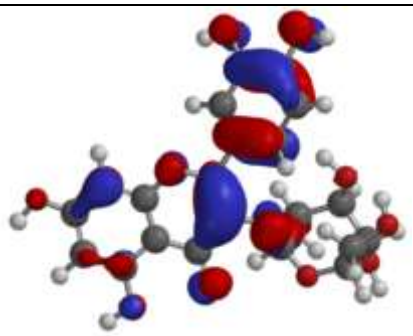	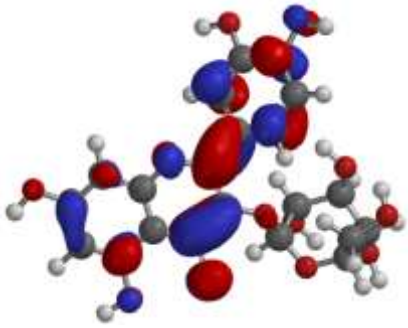
Ligand 4	
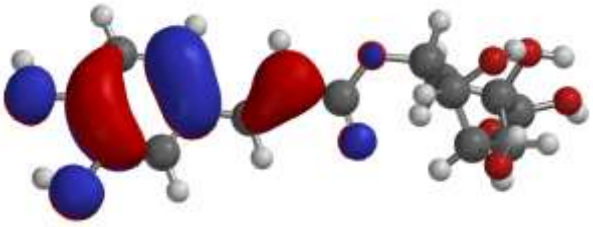	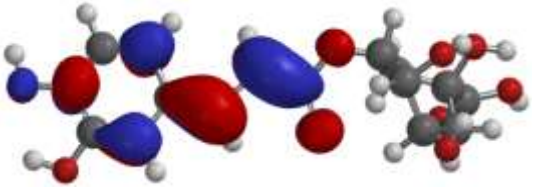
Ligand 10	
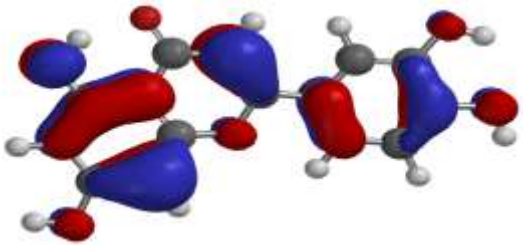	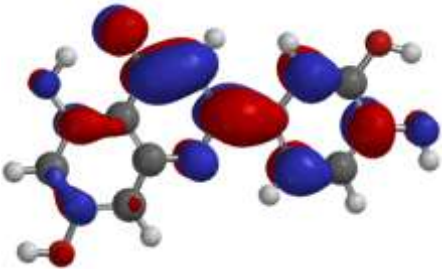

© APR 2026 | IRE Journals | Volume 9 Issue 10 | ISSN: 2456-8880
DOI: https://doi.org/10.64388/IREV9I10-1715885

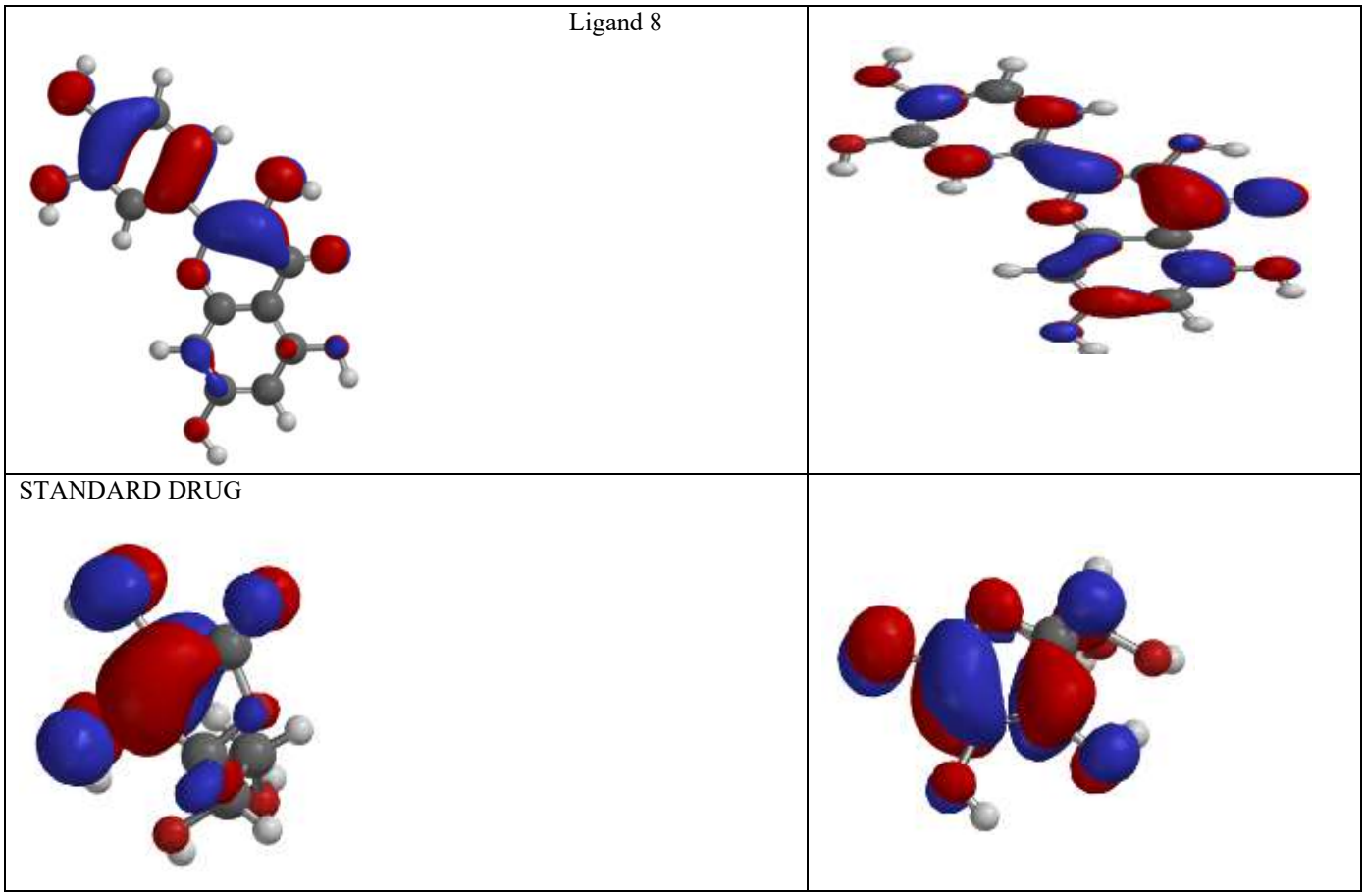

Figure 3. Frontier molecular orbital surfaces of the selected ligands

Table 6: Frontier molecular orbital energies and global reactivity parameters of the selected ligands

S/N	E-HOMO(eV)	E-LUMO(eV)	ΔE	η	Σ	χ	M	Ω
9	-5.93	-1.75	4.14	-2.09	0.48	3.84	-3.84	-3.53
4	-6.05	-1.89	4.16	-2.08	0.48	3.97	-3.97	-3.79
10	-6.12	-1.95	4.17	-2.09	0.48	4.04	-4.04	-3.9
8	-5.45	-1.75	3.70	-1.85	0.54	3.6	-3.6	-3.5
SD	-6.30	-0.76	5.54	2.77	0.36	3.53	-3.53	2.25

The energy of highest occupied molecular orbital (E-HOMO), energy of lowest unoccupied molecular orbital (ELUMO) Energy bandgap (ΔE), chemical hardness (η), chemical softness (σ), global electronegativity (χ), chemical potential (μ), electrophilicity (ω)

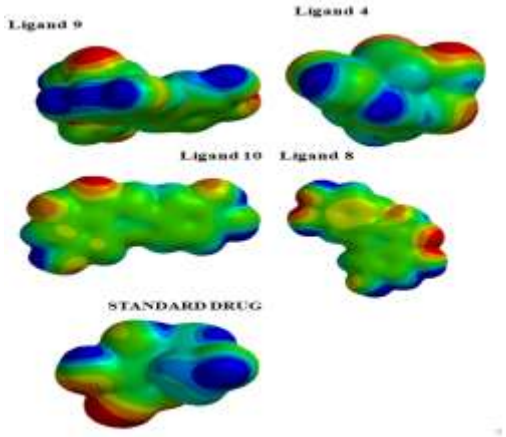

© APR 2026 | IRE Journals | Volume 9 Issue 10 | ISSN: 2456-8880
DOI: https://doi.org/10.64388/IREV9I10-1715885

Figure 4. Molecular electrostatic potential (MEP) of the selected ligands (9,4,10 &8)

3.4 ANTIOXIDANT CAPACITY

The predicted activities and leverage values of the selected ligands are presented in Table 5. These ligands were subjected to quantum chemical calculations in order to investigate their preferred mechanism of free radical scavenge. The molecular structure and carbon atom numbering for these three compounds are presented in Fig. 5

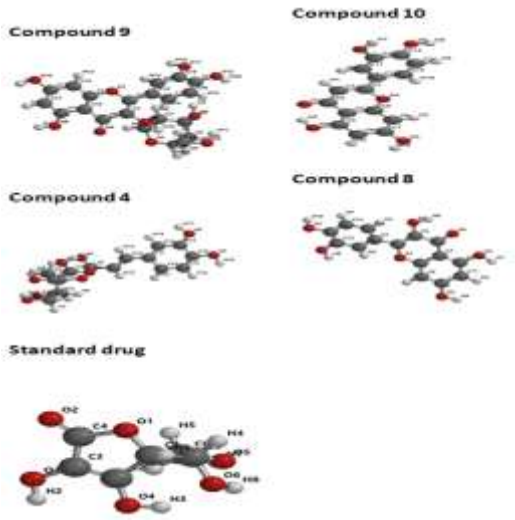

Figure 5: Molecular structure and carbon atom numbering of selected compounds (continued)

3.4.1 Analysis of the HAT mechanism

The computed BDE results for the selected compounds (compound 9, 4, 8 and 10) are presented in Table 4. For compound 9, the 18-OH position has the highest BDE value of 71.928kJ/mol. This high value of BDE could be attributed to the tendency of the hydrogen atom at this position to form intramolecular hydrogen bonds with the carbonyl group of the parent molecule. For this reason, hydrogen atom abstraction is more difficult at this position in comparison to the other positions. Also, HAT occurs more easily at the 19-OH position since it has the lowest BDE value of 45.584kJ/mol. A similar trend is observed for compound 4, where the 14-OH position has the highest BDE value of 32.240kJ/mol due to the possible formation of an intramolecular hydrogen bond with the carbonyl group of the parent molecule. While the 16- OH position has the lowest BDE value of 9.508kJ/ mol. Therefore, HAT occurs more readily at this position. An examination of the BDE results of compound 10 reveals that 5-OH position has the highest BDE value of 95.814kJ/mol due to the possible formation of an intramolecular hydrogen bond with the carbonyl group of the parent molecule. While the 13-OH position has the lowest BDE value of 37.857kJ/mol. For the compound 8, the 9-OH position has the highest BDE value of 71.356kJ/mol while the 15-OH position has the lowest BDE value of 37.666kJ/ mol. From the ongoing discussions, we observe that for Compound 9,4,10 and 8, the lowest values of BDE occurred at the 19-OH, 16-OH, 13-OH and 15-OH positions respectively with values of 45.584kJ/mol, 9.508kJ/mol, 37.857kJ/mol and 37.666kJ/mol. An examination of the BDE values of the standard drug (ascorbic acid) shows that the 2-OH position has the lowest BDE value of 5.382kJ/mol. We can see that from the results; our standard drug has the lowest BDE value compared to the selected compounds at the same level of theory. This implies that

3.4.2 Analysis of SET-PT mechanism

The adiabatic ionization potential (AIP) values for the selected compounds (compound 9,4,8 and 10) were calculated and presented in Table 4.The first step of SET-PT mechanism is characterized by AIP.T he scavenging sites of the selected compounds have AIP values below that of the standard drug which has AIP values of 703.695kJ/mol and 734.613kJ/mol at position 2-OH and 3-OH respectively. This is an indication that the electron-donating ability of these molecules at the various considered sites is stronger than that of the standard drug. For compound 9,4,10 and 8, the lowest value of AIP is found at positions 13-OH (625.525 kJ/mol),16-OH (648.196 kJ/mol),13-OH (693.034 kJ/mol) and 9-OH (622.235 kJ/mol) respectively. For each of these molecules, these sites possess stronger electron-donating ability in comparison to the other sites.

3.4.3Analysis of SPLET mechanism

The ETE values for the selected compounds (compound 9, 4, 8 and 10) were calculated and presented in Table 5. The second step of the SPLET mechanism is characterized by ETE. The ETE results for compound 9,4,10 and 8 recorded lowest values at the position 21-OH,14-OH,12-OH and 13-OH respectively. These are the sites that are most

favoured to undergo electron transfer in the second step of the SPLET mechanism in each of the considered molecules. When the ETE results are compared with those of AIP, the ETE values are found to be lower. Accordingly, the single-electron transfer from the neutral form of the selected compounds to the free radical is less favourable to that from the anionic form

Table 7: Values of BDE, AIP and ETE

S/No.	HAT	SET-PT	SPLET
	BDE (KJ/mol)	AIP(KJ/mol)	ETE(KJ/mol)
9 13-OH	64.833	625.525	170.769
9 18-OH	71.928	-104.827	199.218
9 19-OH	45.584	644.788	-46.631
9 21-OH	-11.317	638.668	111.872
4 14-OH	32.240	668.087	132.311
4 16-OH	9.508	648.196	158.150
10 5-OH	95.814	697.106	162.970
10 7-OH	77.979	-23.030	184.622
10 12-OH	44.722	697.124	139.431
10 13-OH	37.857	693.034	169.169
8 7-OH	64.236	622.240	178.403
8 9-OH	71.356	622.235	191.142
8 13-OH	42.054	633.055	115.342
8 15-OH	37.666	627.790	134.959
SD 2-OH	5.382	734.613	172.272
SD 3-OH	20.787	703.695	138.653

IV. CONCLUSION

This research study proposes some hit compounds as antioxidant drugs by computational approach. molecular docking simulation was successfully used to screen and identify potential hits against 3WGX protein and the four best hit compounds; Compound 9,4,10 and 8 had docking scores of -138.04 kcal.mol-1, -123.399 kcal.mol-1, -117.287 kcal.mol-1 and -116.956 kcal.mol-1 had higher docking scores than the standard drug, ascorbic acid (-81.433 kcal.mol-1). Thus, these compounds are confirmed to have good binding affinity at the binding cavities of the 3WGX protein. Further drug likeness and ADMET screening were performed and these lead compounds also displayed better pharmacokinetics than the standard drug and have also been confirmed to be non-toxic. DFT calculations were also performed to investigate the quantum mechanical parameters which help in understanding the stability of these compounds. Also, the physical and chemical properties of the molecules at the electronic level reveal that they all have higher reactivity than the standard drug. This can be accounted for by the value of their energy band gap (4.1eV, 4.16eV, 4.17eV and 3.70eV for Compound 9,4,10 and 8) which were lesser compared to the standard drug(5.54eV).

The electrophilicity parameter describes these ligands as strong electrophiles (3.53eV, 3.79eV, 3.90eV and 3.50eV for Compound 9,4,10 and 8 respectively) higher than the standard drug(2.25eV). Therefore, from the findings in this research work,it can be concluded that Compound 9,4,10 and 8 can be exploited and modeled into better antioxidants.

ACKNOWLEDGEMENT

The authors gratefully acknowledge the Department of Chemistry, Ahmadu Bello University, Zaria, for providing the academic environment and computational resources that made this research possible. Special appreciation is also extended to the State Key Laboratory of Oil & Gas Reservoir Geology and Exploitation, Chengdu University of Technology, Chengdu, China, for the collaborative support that enriched the scope of this work. The authors further appreciate the contributions of all researchers whose prior work in computational

chemistry, molecular docking, and phytochemistry provided a strong foundation for this study. Finally, sincere thanks go to colleagues and mentors whose valuable suggestions and constructive feedback greatly improved the quality of this manuscript.

REFERENCES

[1] Pizzino, G. and Irrera, N. and Cucinotta, M. and Pallio, G. and Mannino, F. and Arcoraci, V., . . . Bitto, A. (2017). Oxidative stress: harms and benefits for human health. Oxidative medicine and cellular longevity, 2017.

[2] Gulcin, İ. (2020). Antioxidants and antioxidant methods: An updated overview. Archives of toxicology, 94(3), 651-715.

[3] Vishnoi, H. and Bodla, R. B. and Kant, R. and Bodla, R. (2018). Green tea (Camellia sinensis) and its antioxidant property: a review. International Journal of Pharmaceutical Sciences and Research, 9(5), 1723-1736.

[4] Zhang, H. and Tsao, R. (2016). Dietary polyphenols, oxidative stress and antioxidant and anti-inflammatory effects. Current Opinion in Food Science, 8, 33-42.

[5] Kumar, S. and Sharma, S. and Vasudeva, N. (2017). Review on antioxidants and evaluation procedures. Chinese journal of integrative medicine, 1-12.

[6] Shalaby, E. A. and Shanab, S. M. (2013). Antioxidant compounds, assays of determination and mode of action. African journal of pharmacy and pharmacology, 7(10), 528-539.

[7] Saibaba, K. N. (2023). Next generation biosurfactants and their practical application in the food sector Applications of Next Generation Biosurfactants in the Food Sector (pp. 349-360): Elsevier.

[8] Rani, V. and Deep, G. and Singh, R. K. and Palle, K. and Yadav, U. C. (2016). Oxidative stress and metabolic disorders: Pathogenesis and therapeutic strategies. Life sciences, 148, 183-193.

[9] Hussain, T. and Tan, B. and Yin, Y. and Blachier, F. and Tossou, M. C. and Rahu, N. (2016). Oxidative stress and inflammation: what polyphenols can do for us? Oxidative medicine and cellular longevity, 2016.

[10] Habeeb Rahuman, H. B. and Dhandapani, R. and Narayanan, S. and Palanivel, V. and Paramasivam, R. and Subbarayalu, R., . . . Muthupandian, S. (2022). Medicinal plants mediated the green synthesis of silver nanoparticles and their biomedical applications. IET nanobiotechnology, 16(4), 115-144.

[11] Kaurinovic, B. and Vastag, D. (2019). Flavonoids and phenolic acids as potential natural antioxidants: IntechOpen London, UK.

[12] Brogi, S. and Ramalho, T. C. and Kuca, K. and Medina-Franco, J. L. and Valko, M. (2020). In silico methods for drug design and discovery (Vol. 8, pp. 612): Frontiers Media SA.

[13] Abdolmaleki, A. and B Ghasemi, J. and Ghasemi, F. (2017). Computer aided drug design for multi-target drug design: SAR/QSAR, molecular docking and pharmacophore methods. Current drug targets, 18(5), 556-575.

[14] Neochoritis, C. G. and Tsoleridis, C. A. and Stephanidou-Stephanatou, J. and Kontogiorgis, C. A. and Hadjipavlou-Litina, D. J. (2010). 1, 5-Benzoxazepines vs 1, 5-benzodiazepines. One-pot microwave-assisted synthesis and evaluation for antioxidant activity and lipid peroxidation inhibition. Journal of medicinal chemistry, 53(23), 8409-8420.

[15] Inaba, K., Suzuki, M., Kojima, R. (2014) Available at: https://www.rcsb.org/structure/3WGE, https://doi.org/10.2210/pdb3WGE/pdb [Accessed 22 March 2026].